

**Hydraulic Tomography and High-Resolution Slug Testing to Determine
Hydraulic Conductivity Distributions – Year 3**

The University of Kansas
Department of Geology

Carl D. McElwee
Rick Devlin
Brian Wachter

Annual Report
SERDP
Strategic Environmental Research and Development Program
Project # ER1367
December 2007

Also
KGS Open-File Report no. 2008-1

VIEWS, OPINIONS, AND/OR FINDINGS CONTAINED IN THIS REPORT ARE
THOSE OF THE AUTHORS AND SHOULD NOT BE CONSTRUED AS AN
OFFICIAL DEPARTMENT OF THE ARMY POSITION, OR DECISION UNLESS SO
DESIGNATED BY OTHER OFFICIAL DOCUMENTATION

Table of Contents

Background	3
Objective	3
Technical Approach	3
Introduction	4
Theory	11
Field Methodology	18
HRST Techniques	18
CPT Techniques	20
Modeling and Data Processing	23
Simple Models	24
Data Processing	25
Application to Simple Models	28
Application to More Complex Models	28
Vertical Sensor Array	30
MOGs Spring and Summer 2007	32
New Wells Installed	41
HRST	48
MOGs in New Wells	50
Summary and Conclusions	51
References	53
Appendix	
A. Technical Publications	56

Background:

A considerable body of research has shown that the major control on the transport and fate of a pollutant as it moves through an aquifer is the spatial distribution of hydraulic conductivity. Although chemical and microbial processes clearly play important roles, their influence cannot fully be understood without a detailed knowledge of the subsurface variations in hydraulic conductivity at a site. A number of theories have been developed to quantify, in a generic sense, the influence of these variations using stochastic processes or fractal representations. It is becoming increasingly apparent, however, that site-specific features of the hydraulic conductivity distribution (such as high conductivity zones) need to be quantified in order to reliably predict contaminant movement. Conventional hydraulic field techniques only provide information of a highly averaged nature or information restricted to the immediate vicinity of the test well. Therefore, development of new innovative methods to delineate the detailed hydraulic conductivity distribution at a given site should be a very high priority. The research proposed here is directed at addressing this problem by developing techniques with the ability to map 3-D hydraulic conductivity distributions.

Objective:

Since spatial changes in hydraulic conductivity are a major factor governing the transport and fate of a pollutant as it moves through an aquifer, we have focused on the development of new innovative methods to delineate these spatial changes. The objective of the research proposed here is to build on our previous research to develop and improve field techniques for better definition of the three-dimensional spatial distribution of hydraulic conductivity by using hydraulic tomography coupled with high-resolution slug testing.

Technology Approach:

We have been working for a number of years to quantify hydraulic conductivity fields in heterogeneous aquifers. One method we have worked on extensively that shows great promise is high-resolution slug testing. This method allows the delineation of the vertical distribution of hydraulic conductivity near an observation well. We propose to combine this method with another innovative method for investigating the hydraulic conductivity distribution between wells, called hydraulic tomography. We will use an oscillating signal and measure its phase and amplitude through space in order to estimate the hydraulic conductivity distribution of the material through which it has traveled. Our preliminary work has shown that the phase and amplitude of the received signal can be measured over reasonable distances. The high-resolution slug testing results will be used as an initial condition and will provide conditioning for the tomographic inverse procedure, to help with any non-uniqueness problems. Slug test data are most accurate near the tested well and should probably not be extrapolated blindly between wells. Together, slug testing and hydraulic tomography should be more powerful than either one used in isolation and should give the best opportunity to characterize the hydraulic conductivity in-situ by a direct measure of water flow, as an alternative to indirect methods using geophysical techniques.

Introduction

A typical method used to determine fluid behavior in a geologic matrix near a well is a pumping test. Here a pump is installed into a well and groundwater is removed or injected while water levels in surrounding observation wells are monitored. Then the aquifer parameters can be estimated by monitoring changes in water levels at observation wells at some distance. These types of tests are typically large in scale, (Schad and Teutsch, 1994). Another test is an interference test, which is a special pumping test where the pump discharge has a variable rate. Interference tests are conducted by variable production or injection fluid (hydraulic head changes) at one well, and observing the changing pressure or hydraulic head with time and distance at other locations. These tests are valued to estimate flow characteristics *in situ*, but are measures of the aquifer material over large volumes also.

On the other hand, physical cores of aquifer material can be obtained by a variety of drilling methods. These samples can then be tested in a laboratory (i.e., falling or constant head permeability tests) to estimate the hydraulic properties. One advantage to this method is that the sample can be visually inspected. Some disadvantages to this method are that the material is disturbed from its natural environment and the sample is a small representation of the total aquifer.

Another common technique for determining aquifer parameters is to conduct slug tests. A slug test initiates a head change in a well then monitors the response of the aquifer material in order to estimate the hydraulic conductivity (K). Slug testing is usually only conducted in a single well. It is generally accepted that the radius of influence of a slug test is small and only provides a limited view of subsurface

hydrogeologic properties near the well. Traditionally, slug tests have been initiated with the addition into a well of a known volume of water or a physical slug. More recently, pneumatic methods have become popular (Zemansky and McElwee, 2005; Sellwood, 2001; McCall et al., 2000) for multilevel slug testing. Slug tests in low K formations can take very much longer than in material with high permeability. To overcome this, the fluid column in a well can be pressurized and the pressure change with time can be used as a alternative (Bredehoeft and Papadopoulos, 1980).

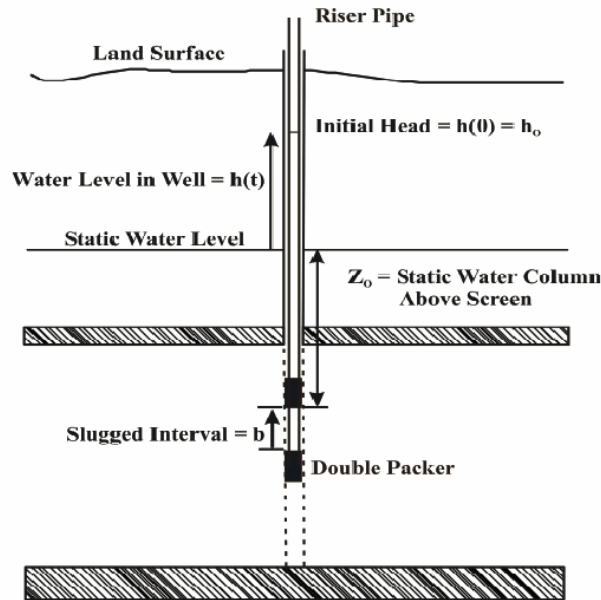


Figure 1. High resolution slug testing equipment deployed in a fully penetrating well.

Typical slug tests are conducted by exciting the entire length of the well screen. Whole well slug testing can provide information near the tested well but it is averaged over the total length of that well's screen. However, aquifers are naturally heterogeneous and whole well slug testing is unable to distinguish areas of high or low K. High resolution slug testing [(HRST), over short screen intervals (Figure 1)] was developed to provide a more detailed vertical profile of K near the tested well. In this research the

HRST interval is approximately 0.5 m; but, stressed intervals as small as 5 cm have been used (Healey et al., 2004). Currently there is no accepted method to bridge the gap between the larger lateral well-to-well averages from pumping or interference tests and detailed vertical estimates of K from HRST. Proposed here is a method to obtain estimates of aquifer parameters at larger radii of influence, while simultaneously maintaining a higher resolution.

Pulse testing is one method of determining fluid flow parameters that is often employed by the petroleum industry. Johnson et al. (1966) published results to experiments conducted in a sandstone reservoir near Chandler, OK. It was found that the new pulse method was as effective as typical interference tests. The transient pressure signal is propagated by *in situ* fluid and is therefore a direct measure of reservoir diffusivity. Other advantages of the pulse method are the ability to distinguish the test from background noise because of its controlled frequency of oscillation and the reduction of down time relative to production. Since 1966, pulse testing has been used to delineate fractures (Barker, 1988; Brauchler, et al., 2001) and to predict water flood performance (Pierce, 1977).

Other pulse test examples include tidal, seismic and oil field methods. The changes in groundwater levels as a result of tidal fluctuations have been well studied (Ferris, 1951; Hantush, 1960) and (Jiao and Tang, 1999). The sinusoidal tidal fluctuations which propagate inland through an aquifer are related to aquifer storativity and transmissivity. Solutions to water level fluctuations induced by seismic waves were presented by Cooper et al. (1965). The pressure head fluctuations controlling water levels are a result of the vertical motion of the aquifer but are dominated by dilation of

the aquifer porosity. An interference test of alternating oil production and shut in time was conducted to determine the interconnectivity of wells in a production field (Johnson et al., 1966). Here the source well is assumed to be a line source in an infinite homogeneous reservoir. The time lag and the received amplitude were used to estimate the average well-to-well transmissivity and storage properties of the reservoir. These oil field methods were theoretically adapted to hydrogeologic characterization by Black and Kipp (1981). Analytical solutions of a fracture responding to a single pulse interference test, a slug of water, was modeled and tested by Novakowski (1989). Straddle packers isolated the fracture and were used to apply the slug of water by being deflated. The duration of these tests was on average 30 min. The sequential pumping or removal of water was used to collect head responses between wells (Yeh and Liu, 2000). In these experiments multiple ray paths were analyzed as a hydraulic tomography experiment. Such experiments show promise in their ability to distinguish lateral and vertical 2-D variations in heterogeneity by changes in the signal over the travel path.

The research presented in this report uses continuous, controlled, sinusoidal pressure signals [the continuous pulse test (CPT)] as a means to estimate vertical profiles of well-to-well averaged hydraulic diffusivity. In this research, the primary method of stimulation of the alluvial aquifer was achieved by pneumatic methods. The column of air within a well was pressurized via an air compressor. A signal generator was used to open and close valves at the well-head allowing air to enter or exit the well. The signal generator produced an adjustable frequency step function, controlling the periodicity of the pulse-testing event. Theoretically, a square wave pressure test is the simplest to conduct because of the instantaneous pressure changes (Lee, 1982). Due to the input air

pressure, the water column in a well will be depressed creating flow through the well screen. This pulse of hydraulic pressure is transferred to the aquifer system based on the diffusivity of the material. As the air column within the well is allowed to return to atmospheric pressure, water will rush back into the well from the aquifer. These fluctuations are periodic and similar to tidal fluctuations acting upon a coastal aquifer system. The governing equations for an aquifer responding to tidal fluctuations were adapted to Cartesian, cylindrical, and spherical coordinate systems describing groundwater flow with sinusoidal boundary conditions, in order to describe the data used in this report.

The period, the phase, and the amplitude of the produced wave can then be measured simultaneously at the source well and at observation wells. Through dispersion, the aquifer material will decrease the fidelity of a step input, retard the propagation, and attenuate the propagating wave front, resulting in a phase lag or shift, and a decrease in the amplitude. The amplitude ratio [received amplitude A_r divided by the initial amplitude A_0] and the phase difference [reference phase ϕ_0 minus the received phase ϕ_r] can then be used to calculate the hydraulic diffusivity (Lee, 1982).

Zero Offset Profile (ZOP, source and receiver at same elevation) data and Multiple Offset Gather (MOG, source location fixed; receiver elevation varied) data were collected at the University of Kansas' Geohydrologic Experimental and Monitoring Site (GEMS), a well-studied shallow semi-confined alluvial aquifer system in the Kansas River floodplain. Line sources equal to the total screen length and point sources isolated by custom bladder packers were used in these experiments. Field data indicate that sinusoidal signals can propagate reasonable distances, and may provide estimates of the

well-to-well diffusivity. Vertical profiles of hydraulic conductivity (K), measured with high-resolution slug testing (HRST) were collected for correlation with the CPT data.

The GEMS area is located in Douglas County, northeast Kansas, along the northern margin of the Kansas River flood plain (Figure. 2). GEMS is in a Pennsylvanian bedrock valley filled with Wisconsin-age glaciofluvial terrace sediments (Schulmeister, 2000). The upper 11 m of sediments are mostly silts and clays and the lower 12 m of sediments at GEMS consists of a fining upward sequence of pebbles, coarse sand, and fine sand, which is underlain by the Tonganoxie Sandstone (Jiang, 1991). Within the sequences of sandy material are lenses of low permeability fine-grained sediments. These clay lenses occur at various elevations and can be up to 1 m thick (Schulmeister, 2000 and Healey et al., 2004). As an aquifer, the Kansas River alluvium is a prolific deposit of unconsolidated sands and gravels. It is a high yielding semi-confined aquifer meeting the needs of agricultural, industrial, and community interests.

Many studies have been conducted at GEMS and many well nests have been completed to various depths with various screen lengths. Porosity, grain size, and K were estimated by laboratory experiments were performed on physical samples of the aquifer material (Jiang, 1991). A single well injection tracer test was used to estimate a K distribution by monitoring the transport of an electrolytic solution (Huettl, 1992). The K distribution in an area of GEMS was also estimated by conducting an induced-gradient tracer test through a multilevel groundwater sampling well field (Bohling, 1999). Direct push bulk electrical conductivity (EC) profiling (Figure 3) and direct push pneumatic slug tests were also done adjacent to the tracer experiment well field (Sellwood, 2001).

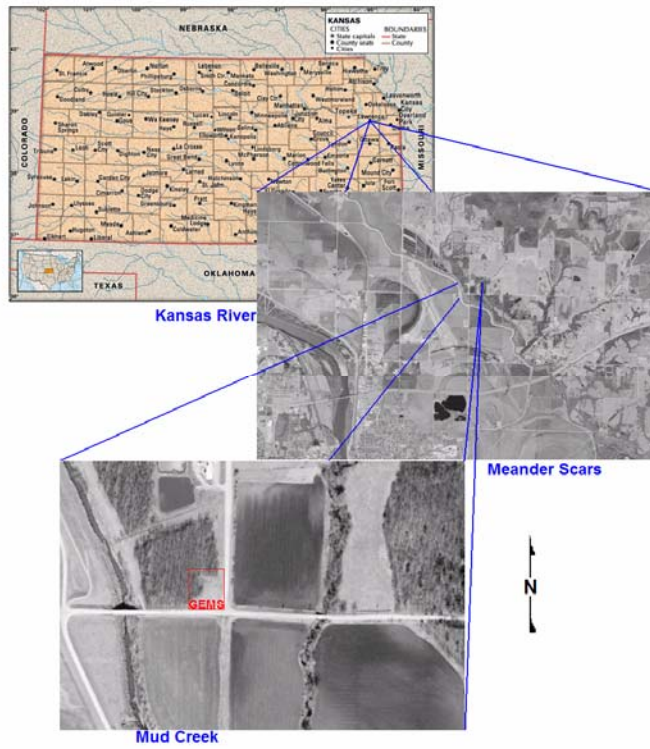


Figure 2. GEMS location map and aerial photographs.

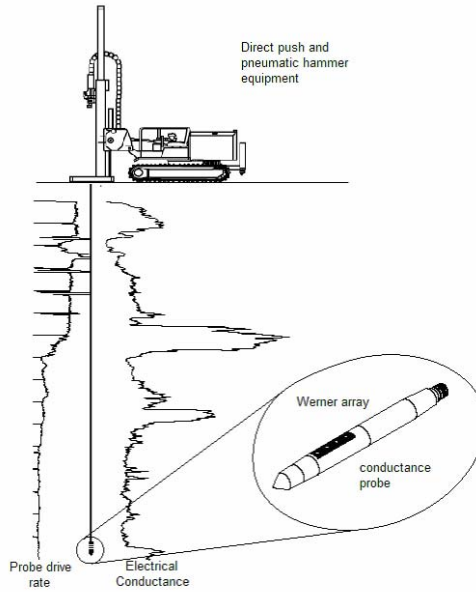


Figure 3. Direct push drilling unit, Electrical Conductance probe, and example profile.

Most recently, HRST K estimates were collected in numerous wells, which were fully screened through the aquifer material (Ross, 2004; Ross and McElwee, 2007). These independent studies and the research presented here all produced estimates of K that can be collected into a database. After compiling this data, vertical and lateral variations of the K distribution are evident. Typically at GEMS, K increases with depth in the sands and gravels, and low K material can be associated with high EC measurements, usually associated with the overlying silt and clay sediments. In most areas at GEMS, “layers” or zones of high K material are apparent in the sand and gravel aquifer.

Theory

Fluid flow in saturated aquifers behaves much like heat flow and can be described by similar equations. Excess pore pressures, matrix permeability, compressibility, and storativity all influence the fluctuations of groundwater levels in response to applied stresses. The excess fluid pressure P_e , above hydrostatic pressure P_s , is related to the total stress on the aquifer σ , and changes the stress $\Delta\sigma$ by

$$(1) \quad \sigma + \Delta\sigma = \sigma_e + (P_s + P_e)$$

The above equation allocates the additional stress to either the aquifer matrix itself (σ_e) or to excess hydraulic pressure, P_e . By changing the hydraulic pressure or hydraulic head, the water levels in an aquifer will also change accordingly. The total hydraulic head (h) hydraulic potential measured in a well is a combination of the elevation head z , and the hydraulic pressure head, P

$$(2) \quad h = z + P/\rho g$$

such that

$$(3) \quad P = P_s + P_e$$

Since the elevation is static, the only dynamic portion of h is due to pressure changes as shown in the following equation

$$(4) \quad \frac{\partial h}{\partial t} = \frac{1}{\rho g} \frac{\partial P}{\partial t}$$

where ρ is the fluid density and g is the acceleration of gravity. Substituting equation (3) into equation (2) the total head measured in a well can also be expressed as

$$(5) \quad h = z + (P_s/\rho_w g + P_e/\rho_w g)$$

Darcy's law states that the discharge Q of a fluid through a porous media depends on the hydraulic gradient (the change in head with distance) $\frac{\partial h}{\partial L}$, and the cross sectional area A .

Darcy's Law is

$$(6) \quad Q = -KA \frac{\partial h}{\partial L} .$$

Darcy's proportionality constant K , now called hydraulic conductivity, is a measure of how easily a fluid will flow through an aquifer. By combining equation (5) with equation (6) the one-dimensional horizontal flow in the x direction q_x is

$$(7) \quad q_x = -K_x \left(\frac{\partial h}{\partial x} \right) = -K_x \left(\frac{\partial}{\partial x} \right) \left[z + \left(\frac{P_s}{\rho g} + \frac{P_e}{\rho g} \right) \right]$$

Assuming that z and P_s are constant, the flow due to excess pressure is

$$(8) \quad q_x = -\frac{K_x}{\rho g} \left(\frac{\partial P_e}{\partial x} \right)$$

Diffusivity is the ratio

$$(9) \quad D = T/S = K/S_s.$$

D is a measure of the ability of an aquifer to transmit changes in the hydraulic head. The following conservation equations, written either in terms of P_e or h , demonstrate the relationship between K , S_s , and D

$$(10) \quad K_x \frac{\partial^2 P_e}{\partial x^2} = S_s \frac{\partial P_e}{\partial t} \rightarrow D \frac{\partial^2 P_e}{\partial x^2} = \frac{\partial P_e}{\partial t}$$

and

$$(11) \quad K_x \frac{\partial^2 h}{\partial x^2} = S_s \frac{\partial h}{\partial t} \rightarrow D \frac{\partial^2 h}{\partial x^2} = \frac{\partial h}{\partial t}$$

The above equations can be generalized to three dimensions. It is the goal of this research to utilize the response of hydrogeologic material to cyclic pressure signals to estimate the D or K distribution in an aquifer.

Groundwater fluctuations near coastal regions have been studied and elementary equations have been developed to associate regional groundwater levels with tidal fluctuations (Hantush, 1960). The basic mathematical description of a one-dimensional transient pressure head signal with sinusoidal boundary conditions $[\sin(2\pi ft)]$ is

$$(12) \quad h(r, t) = h_o e^{-d} \sin(\Phi_o - \Phi_r).$$

The head at some distance and time $h(r, t)$ is the initial amplitude h_o , some decay term e^{-d} , multiplied by the sine of the source reference phase ($\Phi_o = 2\pi ft$) minus the phase shift, Φ_r . The amplitude decay and the phase shift depend on the ability of the aquifer to transmit the sinusoidal signal. Namely, it is the hydraulic diffusivity (D or K/S_s) of the aquifer which influences the hydraulic head measured at some distance and time from the source of a pressure head fluctuation. Three equations for the head response, to the propagation of a sinusoidal boundary condition (causing excess fluid pressure) within a homogeneous

isotropic formation, have been adapted from equation (12). Equation (12) has been extended to various coordinate systems, which are presented below.

Linear Cartesian System

$$(13) \quad h(x,t) = h_o e^{-\sqrt{\frac{\pi f S_s}{K}} x} \sin\left(2\pi ft - \sqrt{\frac{\pi f S_s}{K}} x\right)$$

Cylindrical Radial System

$$(14) \quad h(r,t) = h_o \frac{e^{-\sqrt{\frac{\pi f S_s}{K}} r}}{\sqrt{r}} \sin\left(2\pi ft - \sqrt{\frac{\pi f S_s}{K}} r\right)$$

Spherical Radial System

$$(15) \quad h(r,t) = h_o \frac{e^{-\sqrt{\frac{\pi f S_s}{K}} r}}{r} \sin\left(2\pi ft - \sqrt{\frac{\pi f S_s}{K}} r\right)$$

Where t is time, x or r is the distance from the source, f is the frequency, h_o is the initial amplitude of the pressure head fluctuation at the source, S_s is the specific storage, and K is the hydraulic conductivity. Specific storage is the volume of fluid added or released per unit volume of aquifer per unit thickness, from compression or relaxation of the aquifer skeleton and pores due to changes in stress. The coordinate equations (13, 14, and 15) can be thought of as two parts: the amplitude [AMP] on the right hand side

$$(16) \quad AMP = h_o \frac{e^{-\sqrt{\frac{\pi f S_s}{K}} r}}{r^*}$$

where r^* is the appropriate denominator in equations (13, 14, and 15), and the sinusoidal source phase Φ_o ,

$$(17) \quad \Phi_o = \sin(2\pi ft) .$$

The difference in phase Φ_r between two locations is expressed by the term

$$(18) \quad \Phi_r = -\sqrt{\frac{\pi f S_s}{K}} r = d$$

which is equal to the exponential decay term (d) in equations (12, 13, 14, and 15). Both the amplitude decay and the degree of phase shift depend on the ratio of hydraulic conductivity to specific storage, which is the hydraulic diffusivity (D). Estimates of K may be inferred from equation (18) to compare with other methods if S_s is assumed.

The preceding equations can be used to predict phase and amplitude versus distance for homogeneous systems, where K and S_s are constant. However, for heterogeneous systems where no analytical solutions are available, one must resort to numerical solutions. We postulate that perhaps these relatively simple formulas presented above can be used to analyze the data for heterogeneous cases by using a distance weighted average for the K in the above equations. The premise is that the following replacement in the above equations might work.

$$(19) \quad \sqrt{\frac{\pi f S_s}{K}} r \Rightarrow \sum_{i=1}^I \sqrt{\frac{\pi f S_s}{K_i}} (r_i - r_{i-1})$$

The index (I) indicates the present location of r; so, the summation continues up to the present location of r and terminates at that point.

As indicated above, one must resort to numerical methods to calculate the phase and amplitude relations with respect to distance for heterogeneous cases where K and S_s are changing with distance. We have developed numerical models for calculating the amplitude and phase in the presence of heterogeneity for Cartesian, cylindrical, and spherical coordinate systems. It was shown in the previous year's annual reports (Engard

et al., 2005; 2006) that the simple replacement proposed by equation (19) can be used to simplify the inversion for K in certain cases. This year we have extended that investigation to the spherical heterogeneous system.

As shown above, the homogeneous equations can be used to predict K based on the measurable amplitude decay and phase shift. However, the values obtained for the horizontal rays must be interpreted as spatially weighted averages over the horizontal distance between wells. Equations (14) and (15) represent the two experimental approaches utilized in this research. The cylindrical radial equation (14) describes the behavior of the excitation of a relatively long and small radius section of screen and is considered to behave like a line source. Fully penetrating wells are often constructed at GEMS. Any test where the total screen length is excited is termed a whole well test. The spherical radial equation (15) is a representation of the point source geometry, where the excited length of well screen is relatively short. To achieve this, either a partially penetrating well with a relatively short screen length or a straddle packer apparatus must be used. A straddle packer is a double inflatable packer arrangement, which isolates a centralized interval. It would be advantageous if the packer apparatus can be deployed down typical 2 inch (5.08 cm) observation wells; so, considerable effort has been expended to design such packers for this research.

Previous studies have shown that a line source allows for higher energy input, higher amplitudes, and increased signal propagation (Black and Kipp, 1981). A line source can create multiple ray paths to the receiver, decreasing the resolution and only approximating gross K distributions. High K material can also preferentially propagate excess pore pressures generated by a line source, which will induce a vertical gradient

and cross-flow within the aquifer. Depending on the 3-D heterogeneity distribution, this cross-flow will alter the receiver signal, similar to a weighted average, again decreasing the resolution. Even high amplitude line source signals decay rapidly in the subsurface. Most of the decay is due to the exponential term in equations (14 and 15). In addition, the radial distance between source and receiver wells will cause further decay (the cylindrical or line source will additionally decay by the inverse square root of r [equation (14)] and the spherical or point source will decay by the inverse of r [equation (15)]). These additional amplitude decay effects are due to wavefront spreading loss. However, the point source arrangement may increase the resolution of the K distribution profile because of fewer ray path possibilities.

The common component of the amplitude decay and the phase shift is $\sqrt{\frac{\pi f S_s}{K} r}$; therefore, it is possible to compare the phase data to the amplitude data (after correcting for spreading loss). Using aforementioned assumptions, estimates of K can be obtained through algebraic manipulation. However, this method does not give a specific value for K , but rather an average ratio of S_s/K for the signal travel path from source well to receiver well. Simple theory presented here indicates that the phase and the corrected amplitude ratio should vary linearly with $\sqrt{\frac{S_s}{K}}$ and distance (r) from the source well.

Therefore, average parameters between well pairs may be estimated. Further, if multiple source and receiver offsets (relative to their elevations) are used, multiple diagonal ray paths may be recorded (Multiple Offset Gather, MOGs). This type of testing is called hydraulic tomography (Yeh and Liu, 2000; Bohling et al., 2003), and can give more detailed information about hydraulic properties between well. In the first phase of this

project we concentrated on horizontal rays where the source and receiver are at the same elevation (Zero Offset Profiles, ZOP). A ZOP survey is the simplest tomographical survey to conduct and process, but can only give information on average horizontal aquifer parameters. During the second and third years of this project we have started collecting diagonal ray path data (MOGs). These data do show effects of heterogeneity in K. Therefore, we continue to expend considerable effort trying to find the optimum method of processing this field data.

Field Methodology

Recent studies at GEMS have utilized custom-built straddle packers (McElwee and Butler, 1995; Zemansky and McElwee, 2005; Ross and McElwee, 2007), and pneumatic slug testing technique techniques (McElwee and Zemansky, 2005; Sellwood, 2001; and Ross and McElwee, 2007). In this work custom made packers are used to isolate a zone for testing. This testing may either be high resolution slug testing (HRST) or cross-hole measurement of relative amplitudes and phases for hydraulic tomography .

HRST Techniques

The aquifer material at GEMS exhibits linear and non-linear responses to slug testing (Figure 4). The response of the aquifer material to the slug can be dampened such that water levels in a well return to static head conditions with time in a smooth non-oscillatory curve. However, the aquifer can be underdamped and the water levels will oscillate, decaying with time, until pre-test conditions are reached (Van Der Kamp, 1976). Theoretical advances, presented by McElwee and Zenner (1998) and McElwee (2001, 2002), have made analysis of nonlinear behavior practical and meaningful. The

mentioned slug tests are localized tests; but, continuous layers of geologic material between tested well pairs should correlate with HRST data from each well in the well pair.

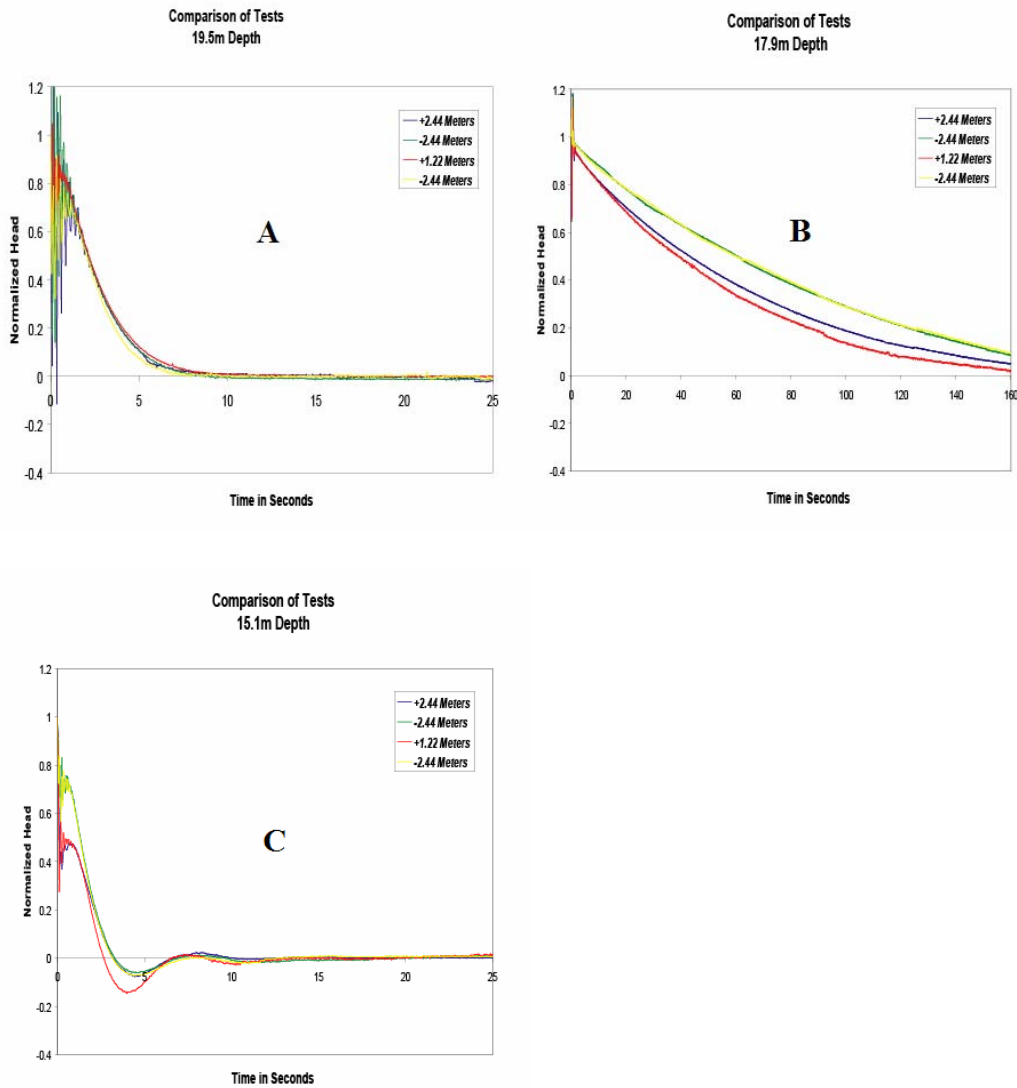


Figure 4. Three examples of slug tests performed at GEMS. Graph A displays no head dependence and behaves linearly. Graph B shows a dependence on the initial slug height and direction. Graph C is oscillatory and has some nonlinear characteristics.

CPT Techniques

The Continuous Pulse Test (CPT) is an exploratory method for extending slug test results between well pairs by propagating a sinusoidal signal. The distance between wells in pairs tested and analyzed with the CPT method in this research have ranged from 3 to 11.5 m. The instrumentation's ability to discern signal from noise may be a limiting factor at greater distances. As with most geophysical techniques, the equipment set up time can consume considerable time in the field. The pneumatic CPT method takes slightly longer to perform than the typical high resolution slug test.

An air compressor is used to supply the driving force behind the CPT method and it is connected to an apparatus attached to the top of the casing at the well (Figure 5).

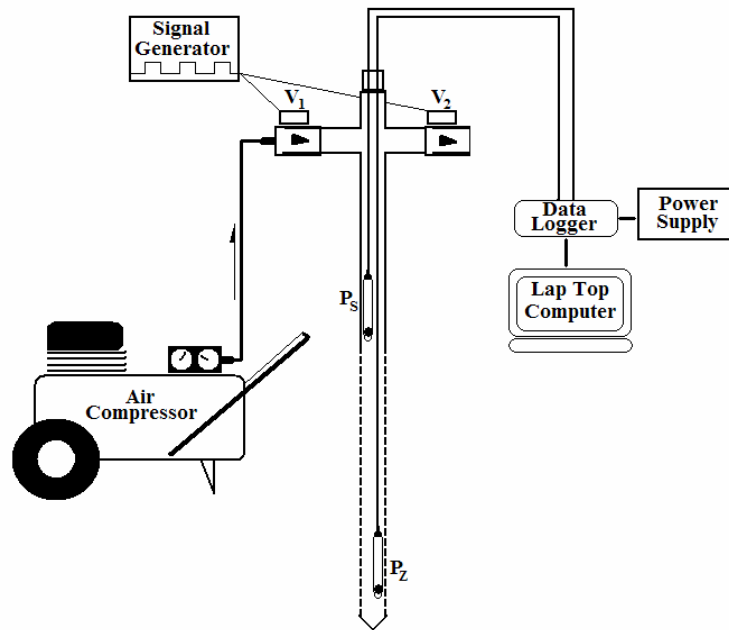


Figure 5. The pneumatic CPT equipment set up for a line source configuration. A signal generator opens and closes valves (V₁ and V₂) to control the flow of air supplied by the air compressor. The pressure transducers record the amplitude and phase at depth P_z and a reference location P_s. This setup can be easily modified for a point source configuration by using a double packer to isolate the stressed interval.

A signal generator is used to power servo-controlled valves on the apparatus, which allows air pressure to be increased in the well or to be released to the atmosphere. Increasing pressure depresses the water column, releasing the air pressure allows the water column to rebound. A single pulse of pressure is a slug test, while stacking them one after another, will create a CPT. The frequency and amplitude of the CPT data should be adjusted to give optimal results (Engard et al., 2005, Engard, 2006).

Surveys were done in the form of multiple offset gathers. For a MOG, a packed off source excitation interval with a transducer is kept at a fixed depth in the source well while another packed off receiver interval with a transducer is moved throughout the entire screened interval of the receiver well. For this study, measurements were usually taken in 0.30 m (one ft) intervals (Sometimes 1.0 m or three ft intervals were used). Once measurements were collected between one source location and all the receiver locations, the source was moved by 0.30 m and measurements were again collected at all the receiver locations. The process was repeated until rays had traveled from every location in the source well to every location in the receiver well (Figure 6). The collective examination of these multiple ray paths forms the tomographic study.

Initially, a single-channel receiver was used in data collection. However, a multi-level receiver with five pressure transducers was later constructed to expedite data collection. The pressure ports were located approximately 1 m apart isolated on either side by packers measuring approximately 0.6 m in length. The main advantage of this apparatus is that it allows efficient collection of multiple MOGs, which are needed for tomographic surveys.

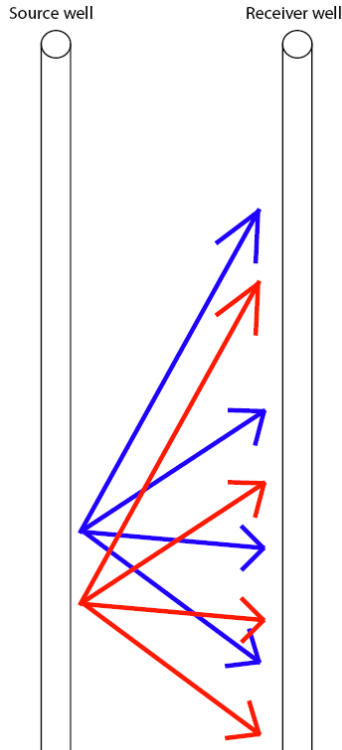


Figure 6. MOG setup for the tomographic study.

The MOG data taken from a well pair should produce a parabolic phase shift curve due to the path lengths of the rays. Path lengths are greater for more distant offsets (Figure 6). Larger phase and amplitude changes occur at these larger offsets. If the source is in the middle of the well, the greatest distance and therefore greatest change in amplitude and phase should occur when the receiver is at the top or bottom. The shortest distance is when the source and receiver are at the same depth. The general shape should be a parabola with distortions due to heterogeneity. When the source is at the top, the shortest distance is to the receiver location at the same depth and the greatest distance is to the receiver location at the bottom of the well. The curve should therefore have a half-parabola shape when the source is at the top of the well. The same is true when the

source is at the bottom of the well. Examples of these parabolic shapes are shown in Figures 7 and 8 of the following section on modeling and data processing.

Pressure transducers were used to monitor pressure head fluctuations in both the source well and at the observation wells. The data were collected from the pressure transducers by a data-logger and stored on a field computer for later analysis. Data were typically recorded at a 20 Hz sampling rate, which provided sufficient temporal resolution. The field computer and data logger allowed real-time monitoring of the CPT records.

Modeling and Data Processing

As presented earlier in this report it is postulated that perhaps a spatially weighted average K value [equation (19)] could be substituted into the homogeneous analytical solution [equation (15)] as an approximation to the heterogeneous case. We have written a program that assumes straight ray paths between the source and receiver and performs a spatially weighted calculation for K for a given raypath in a heterogeneous system, which can be substituted into the analytical solution expressions to calculate the expected phase and amplitude. Since no analytical solutions exist for arbitrary heterogeneous systems, we must resort to numerical modeling to check this approximation. Modeling studies were performed to compare results from the spatially weighted ray-tracing method with those from a numerical model.

Simple Models

The first model used three layers each with a thickness of 3.66 m (12 ft). K values were chosen as 0.00183 m/s (0.006 ft/s) for the top and bottom layers and 0.000915 m/s (0.003 ft/s) for the middle layer. The K values were chosen to approximate those found in the sandy region of the GEMS aquifer. Deviation between the two curves occurs at the lower boundary between layers and at the upper boundary due to boundary effects. The numerical model uses a barrier boundary rather than assuming an infinite solution, so the boundary effects are expected. Aside from the slight deviations at the boundaries between layers, the two curves are very similar (Figure 7).

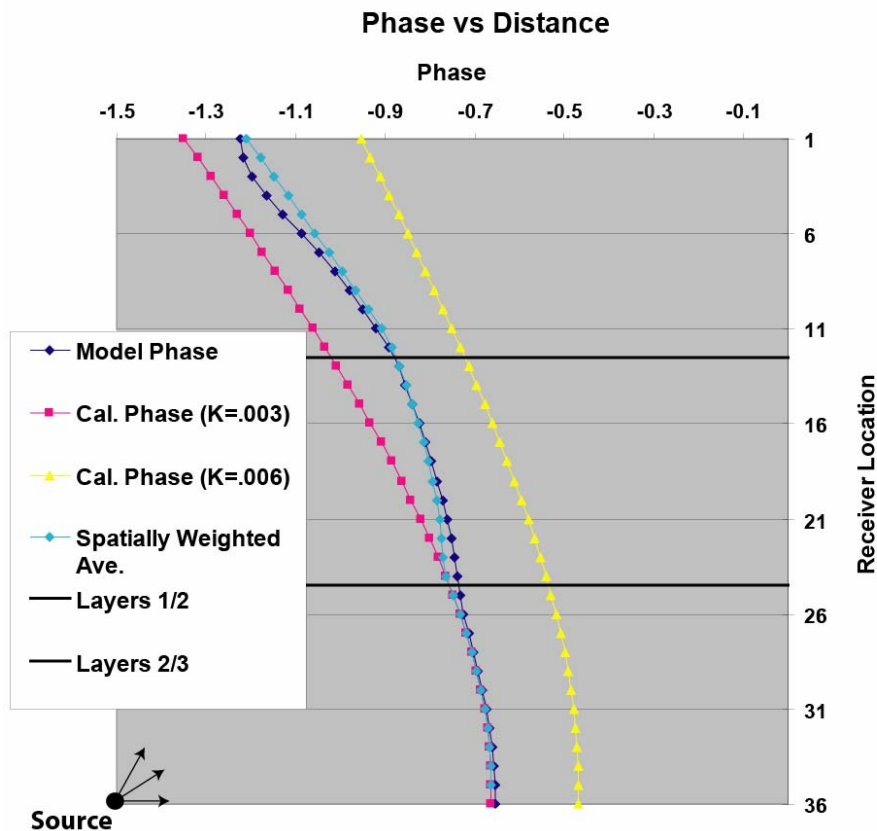


Figure 7. A comparison of phase values from a numerical model, two homogeneous analytical solutions, and the spatially weighted raytrace average for three equally sized layers.

After examining the case of three equal layers, the middle layer was collapsed to examine the resolution of the model. The middle layer was reduced to 0.91 m (3 ft), with the same K values mentioned in the previous example. Once again, the spatially weighted ray-trace method is in good agreement with the numerical model except for some boundary effects, as shown in Figure 8 below.

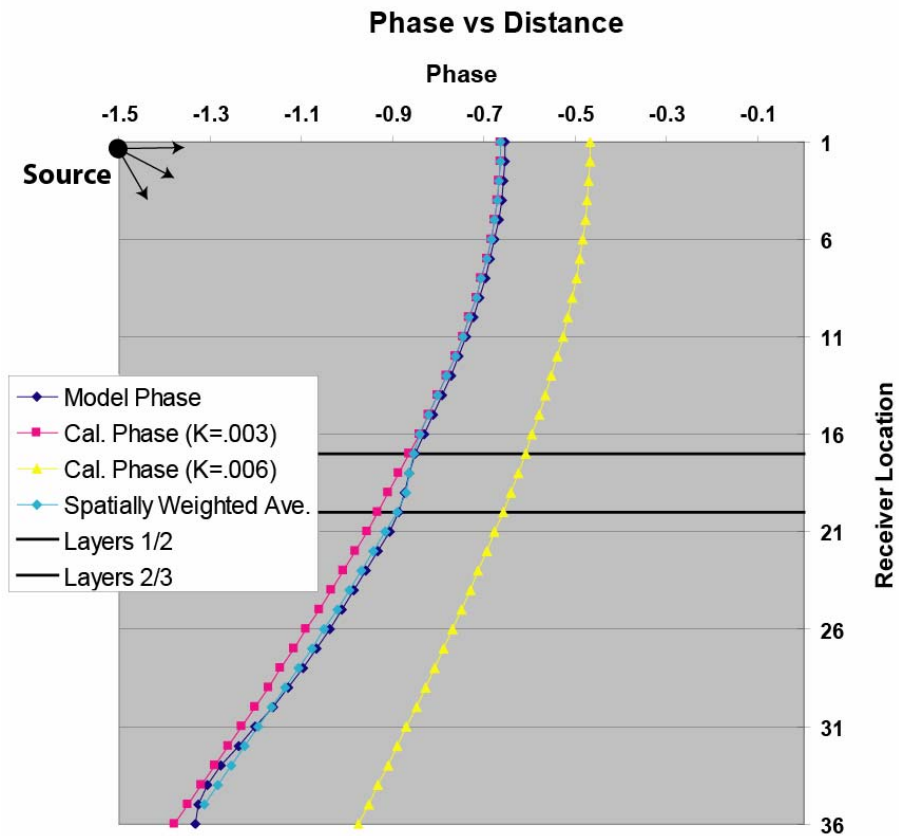


Figure 8. A comparison of phase values using a numerical model, two homogeneous analytical solutions, and the spatially weighted ray-trace average for a thin middle layer.

Data Processing

We have shown examples of phase records for a single source being received at multiple receivers in the previous figures. If several of these phase records are combined

into one data set they can be inverted to obtain the hydraulic conductivity distribution. This is the essence of hydraulic tomography and one would expect the definition and resolution of the calculated hydraulic conductivity distribution to depend on the number of records and the distribution of raypaths. In general, one would expect better results for more records and a greater uniform density of raypaths. In the usual hydraulic tomography inversions one must use nonlinear least squares fitting and iterate for the best fit. This involves running the numerical hydraulic model for the aquifer many times, which is time consuming and computer intensive. The procedure that we are investigating involves the spatially weighted raytracing method. For a given set of raypaths the path lengths through each zone must be computed only once. The phase is then given by multiplying the path length in each zone by a coefficient containing K . This procedure gives a set of linear equations to solve for the coefficients, which in turn may be solved for K . No iteration is required since the equations are linear. The net result is that the procedure is very fast.

Data processing to determine the phase of a sinusoidal signal after it has propagated through a heterogeneous region of aquifer is accomplished by a program written in Visual Basic by Carl McElwee. Different versions have been written for ZOP data and MOG data. MOG data requires several receiver locations be analyzed for the same source location. The signal input to the processing program can be either theoretical output from a numerical model or experimental field data. The program fits sine waves to the data and generates plots of the amplitude ratio as well as the phase shift between the source and receiver, both plotted against receiver location. The program analyzes data for a single source location at a time. The amplitude ratio between the

source and receiver, as well as the phase shift between source and receiver, should both nearly plot as parabolas or half-parabolas for the homogeneous case. Heterogeneity will cause deviations from this parabolic shape. If the source location is near the middle of the well, the shape will be a full parabola, and the shape will only be half a parabola if the source is near either the top or bottom of the well. The shape should be perfectly parabolic assuming no change in aquifer material, so any deviations from the overall parabola must be due to changes in K .

We have implemented a least squares fitting procedure using Singular Value Decomposition for the matrix solution. The SVD, or Singular Value Decomposition, program performs a least squares fitting inversion from phase values to K values using a set of linear equations. The equations do not require iterations because they are linear. If we have m raypaths through the heterogeneous media, then m equations can be written for the phase change or amplitude ratio. Each equation will have n unknowns that correspond to the K values of n regions the ray propagated through. These equations may be expressed in matrix form with the matrix G . The SVD method divides G , an m (data space dimension) by n (model space dimension) into the following equation:

$$G = UWV^T$$

where U is an m by m orthogonal matrix, W is an m by n diagonal matrix with nonnegative diagonal elements known as singular values, V is an n by n orthogonal matrix, and the T superscript indicates that it is a transpose matrix (Aster et al., 2005). Solution by Singular Value Decomposition gives the estimates of K in the n heterogeneous regions of the aquifer.

Application to Simple Models

The output from the numerical model with three layers, whose center layer was collapsed to three ft (See Figure 8) was used for input to the inversion algorithm. Records for three source locations at the top left, middle and lower left were used for a total of 99 ray paths. The error in K for the thin middle layer was about 2.7%, while error in the thicker upper and lower layers was less than 1.5%. Random error of 5% of one phase cycle was added to the numerical model data and the same 99 ray paths were inverted again several times for differing random errors. In the presence of noise, the average error for the 3 ft middle bed was 13.4%, while the average error in the thicker upper and lower beds was still less than 1.5%. These results imply that the spatially weighted ray-trace method works very well and that layers of about one m (3 ft) thickness can be resolved.

Application to More Complex Models

Theoretical values of phase and amplitude were run through the data processing programs before applying the programs to field data. The synthetic data set had no error built in. A model was set up with 6 elements in the x direction and 10 elements in the z direction, as shown in Figure 9. This would represent the cross section between a source and receiver well. The horizontal distance was 19.2 ft and the vertical distance was 30 ft, which is similar to typical distances used at the GEMS field site. With this choice of model dimensions, each element in the model is about one meter (3-4 ft) on a side. The ray-tracing program was used to generate 100 rays going through those 60 elements; each element can represent a different K value. Ray paths shown in Figure 9 are conceptual

and do not represent the full spread of rays. Inverse problems are known to be unstable for many situations, so we decided to investigate the situation for our case. Instability problems resulted due to a difference in ray path density. The ray path density is highest in the center of the region, so there is less resolution at the top and bottom of the modeled area. The problem can be avoided by having spatially variable element sizes across the model. The top row of elements was combined into a single element and the bottom row was also combined into a single element, reducing the 60 element model to a 50 element model shown below. After combining the elements in those two rows, the model became stable and the remaining cross section could be resolved into blocks of distinct K values about one meter on each side. The standard deviations on the K values were very low, implying that the inversion was almost perfect for the data with no noise.

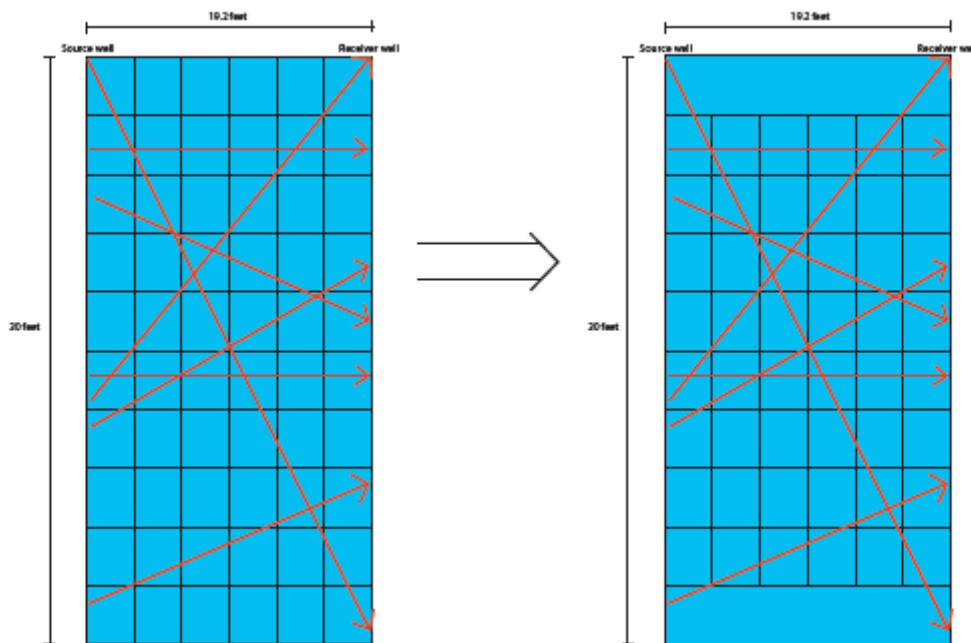


Figure 9. The 60 element model on the left was reduced to the 50 element model on the right to fix instability issues.

Random error was introduced to the 50 element model to approximate noise found in the field. A random number generator was used to add +/- 5% error to the phase data, and the solution for some of the elements in the model became unstable. Although the majority of the K values were reasonable, the K values in a few of the elements were one or two orders of magnitude different than those in the same elements in the model with perfect data. The 50 element model was then reduced to a 40 element model by combining the second row from the top into a single element and the second row from the bottom into a single element. Although instability still persisted, fewer elements were unstable and the magnitude of errors was decreased as compared to the 50 element model. We are working on refining the model to retain stability across all elements in the presence of this random error.

Vertical Sensor Array

We continue to improve the design of the vertical sensor array. Moving the receiver location to many discrete locations along the receiver well screen is very time consuming. To speed this process up, we designed a vertical sensor array with five pressure transducers and six packers. Each transducer is isolated by packers above and below, to allow measurements to be made on a 0.3 m (1 ft) section of the receiver well screen. The transducers are located every 0.91 m (3 ft) along the array, with 0.6 m (2 ft) length packers between. The array may be moved up in 0.3 m (1 ft) increments two times to allow uniform coverage of the first section of the screen at 0.3 m (1 ft) increments. Nearly complete coverage of the 11 m screen can be achieved by pulling the vertical sensor array 3.9 m (13 ft) and repeating the sequence described above. In this

way by recording 6 records with the vertical sensor array, it is equivalent to 30 records with the single receiver setup. This increases the speed of data collection in the field.

However, in the first year of this project, the initial choice of pressure transducer model was not robust enough, resulting in multiple transducer failures. In the second year of this project we tried a different set of transducers with somewhat better results. We collected some data from that apparatus but continued to have some transducer failures. This year we redesigned the vertical sensor array to use larger pressure transducers, which were specifically designed for submerged water level measurements. The first time out we had several nitrogen leaks in the plumbing for inflating the packers. It turned out to be failures in some of the brass fittings, which had been carried over from the earlier design. Replacement of those failed items fixed the leakage problem. The new design seems to work well and we have collected several cross-well surveys with it. Pictures of the new design are shown below in Figure 10.



Figure 10. Vertical sensor array.

MOGs Spring and Summer 07

MOGs were collected in the fall of 2006 with the single-channel receiver. HT-3 was used as the source well and HT-1 was used as the receiver well. Due to the time involved for a complete survey with the single-channel receiver, only five MOGs were collected. The five were chosen at varying depths to attempt to roughly characterize the well as a whole. The maximum range of measurement in the well ranges from a depth of 12.31 m (40.4 ft) to a depth of 21.15 m (69.4 ft). The maximum depth is limited by the

total depth of the well and the minimum depth is limited by attenuation from the overlying clay material. MOGs were collected at depths of 14.11 m (46.3 ft) (Figure 11), 15.33 m (50.3 ft) (Figure 12), 16.55 m (54.3 ft) (Figure 13), 17.47 m (57.3 ft) (Figure 14), and 18.53 m (60.8 ft) (Figure 15). The target depth for the final MOG was 18.68 m (61.3 ft), but material had filled in the bottom of the well. The well was purged in the spring of 2007 to remove this extra material. These first five MOGs were repeated in the spring and summer of 2007 with the vertical sensor array for comparison to the single-channel receiver data.

Shortly after putting the equipment in the wells, a series of nitrogen leaks were discovered in the vertical sensor array. In the field, gas could be heard leaking from the receiver and water was being pushed out of the top of the receiver well when the nitrogen was turned on. A full nitrogen tank only lasted for at most two source locations with complete receiver locations. The equipment was pulled from the wells after completing the HT-3 to HT-1 well pair and taken back to the lab for repairs. Lab tests indicated nitrogen leaking from the inflation plumbing connecting the packers to the nitrogen tank. The plumbing system was redesigned to eliminate some plastic tubing and replace it with copper tubing. In addition, some brass fittings had failed and were replaced. On the outside of the vertical sensor array, some of the packers were leaking slowly under the bladder clamps, so clamps were added or replaced as needed to the ends of the packers. This seemed to fix the leak problem; resulting in a much slower rate of usage of nitrogen in the field.

The phase shifts between source and receiver transducers for each MOG are presented in Figures 11 to 15 below. The delta phase values between source and receiver

from spring 2007 match closely with those taken in fall 2006. The curves are different at each source location, but the results within any given source location are similar enough to assume that the vertical sensor array is functioning properly. The MOGs shown below taken with the vertical sensor array were acquired from the bottom to the top of the well in terms of acquisition sequence. It seems that the later 2007 records are getting noisier due to a worsening of the nitrogen leak. However, the results generally show good reproducibility.

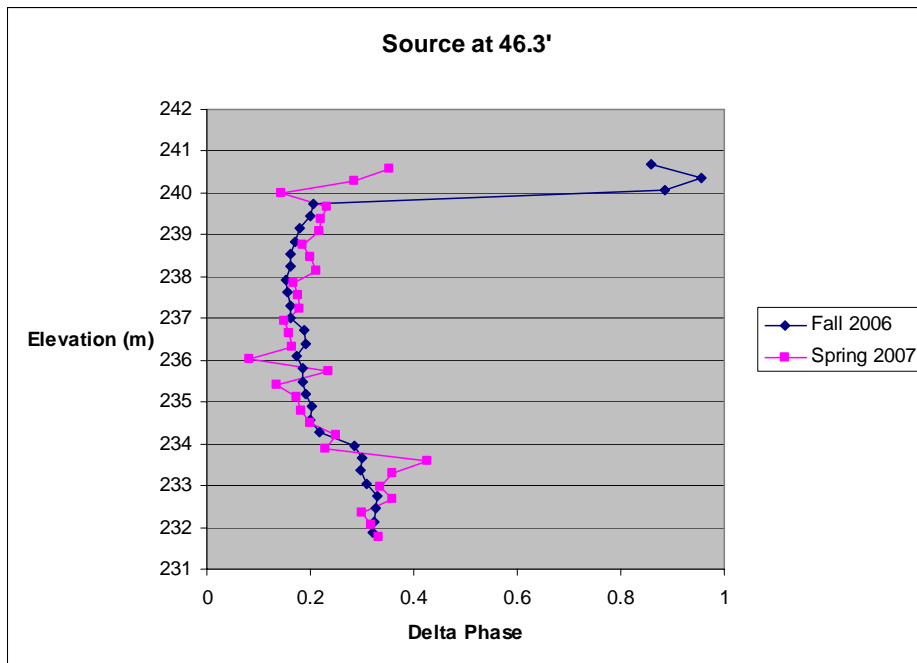


Figure 11. Comparison of fall and spring MOGs from a source location of 46.3 ft.

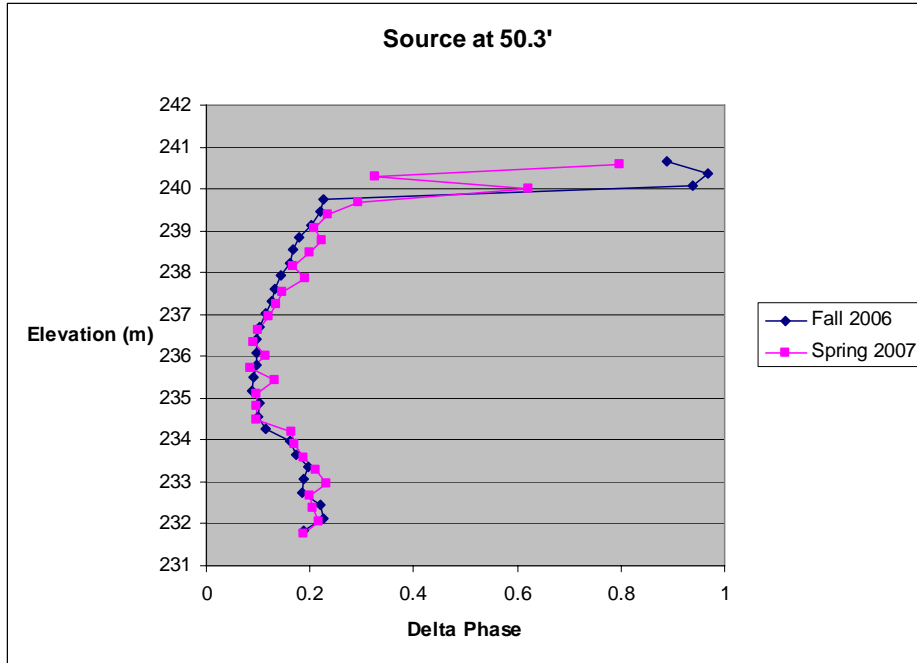


Figure 12. Comparison of fall and spring MOGs from a source location of 50.3 ft.

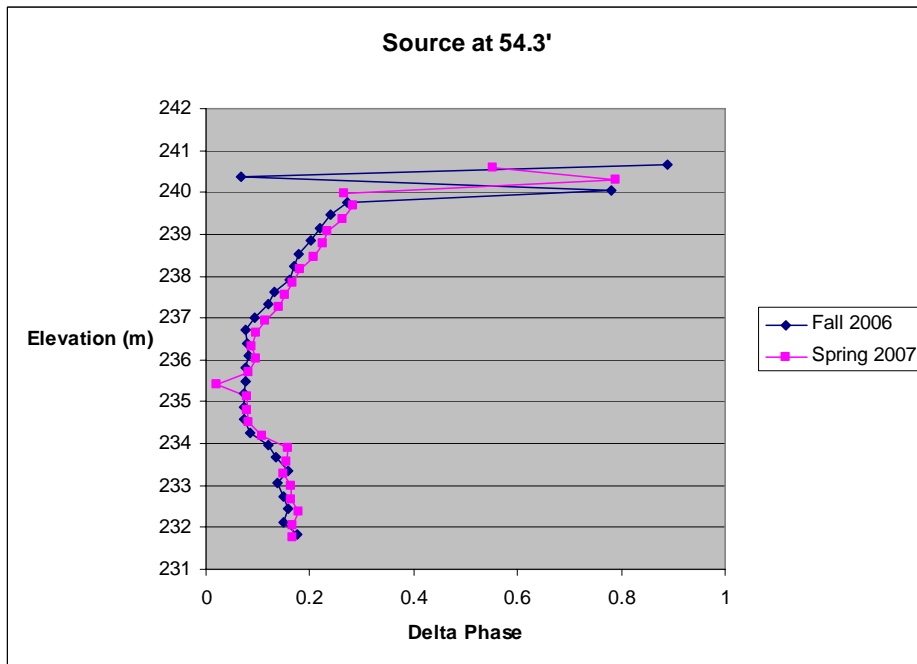


Figure 13. Comparison of fall and spring MOGs from a source location of 54.3 ft.

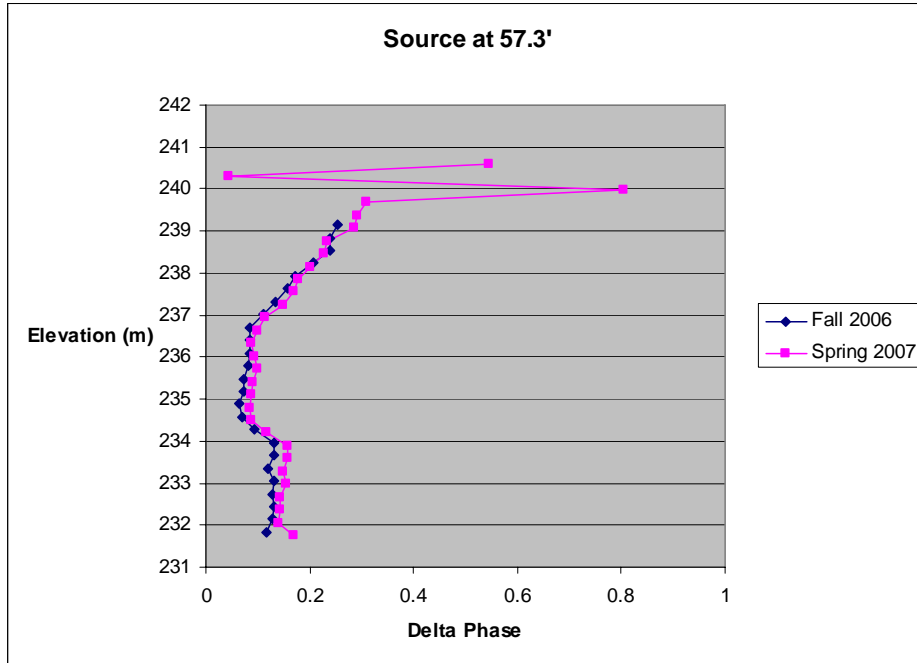


Figure 14. Comparison of fall and spring MOGs from a source location of 57.3 ft.

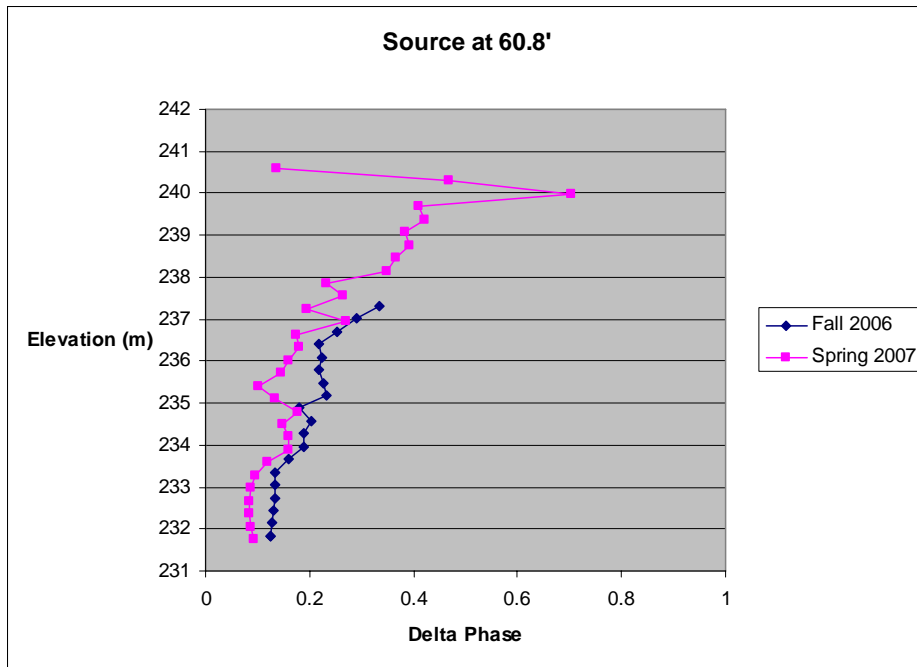


Figure 15. Comparison of fall and spring MOGs from a source location of 60.8 ft.

Once the multi-level receiver had been repaired, it was taken back to the field with HT-3 still as the source well and HT-2 now as the receiver well. A complete survey of this well pair was collected. No leaks could be heard and no water flowed out from the top of the well. A tank of nitrogen lasted for several source locations compared to at most two source locations before, so data collection became much more efficient. The data also seemed to have considerably less noise, as shown in Figures 16 and 17.

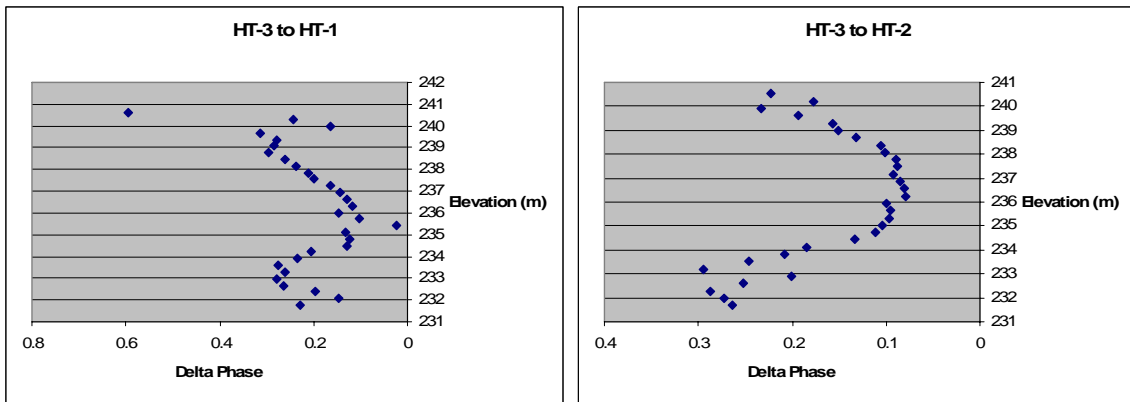


Figure 16. Comparison of parabolas from the middle of the screened interval before fixing leaks (left) and after (right).

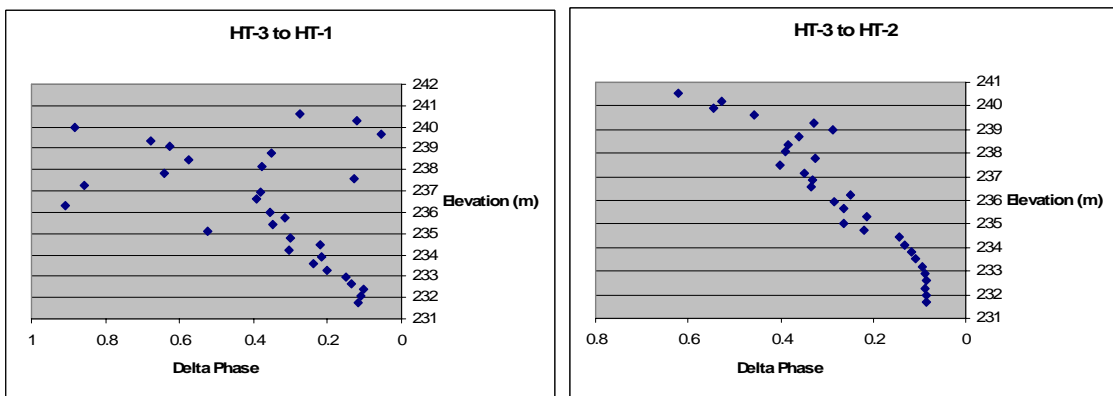


Figure 17. Comparison of half-parabolas from the bottom of the screened interval before fixing leaks (left) and after (right).

The straight-raypath model and SVD inversion programs initially led to unstable results when used on field data. The dimensions were slightly different than with the theoretical data, but the side of each element was still roughly one meter. The initial 36 element model had 4 elements in the x direction and 9 elements in the z direction. The top row of elements was combined into a single element, and the bottom row was also combined into a single element. Instability problems still persisted, so the second row from the top and the second row from the bottom were each combined into single elements. After combining the first and last two rows, the model became stable and the remaining section could still be resolved into blocks of about one meter on each side.

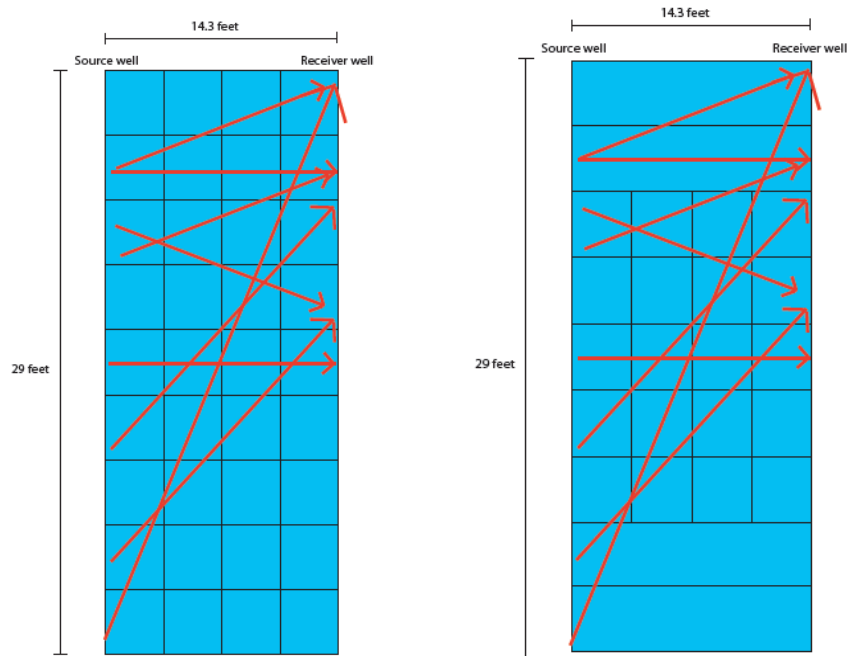


Figure 18. The 36 element model on the left becomes stable when reducing it to the 24 element model on the right.

The field data used for analysis had HT-3 as the source well and HT-2 as the receiver well. This particular well pair was chosen because the data were collected with the multi-level receiver after repairing a series of nitrogen leaks. The data from this well

pair was therefore assumed to have the least amount of error. Although the current inversion routine is stable for the 24 element model, the results do not seem to be very accurately representing the inter-well region, because of a wide variation in the identified values of K . The inverse problem is well known to be a mathematically difficult problem with which to deal. Generally, one must use other known information to condition the inverse. We have not yet done that. We have a very good source of independent data for K in the high resolution slug test data for each well. Research into conditioning the inverse solution will be an area of work in the upcoming months. In the meantime, the SVD program was run with the ray path data for just the horizontal rays. These are essentially zero offset profile (ZOP) data. In a ZOP, the source and receiver are both moved vertically, but they both remain at the same elevation as they are moved. The resulting K values are only horizontal averages, since multiple blocks in the horizontal can not be resolved with horizontal ray data. The resulting K values produced by the program are very similar to those obtained from high resolution slug tests and continuous pulse tests taken in previous years for this well pair. The results are shown in Figure 19. There is good consistency between the data sets. More complete processing of the entire diagonal ray path data set is an area of continuing research.

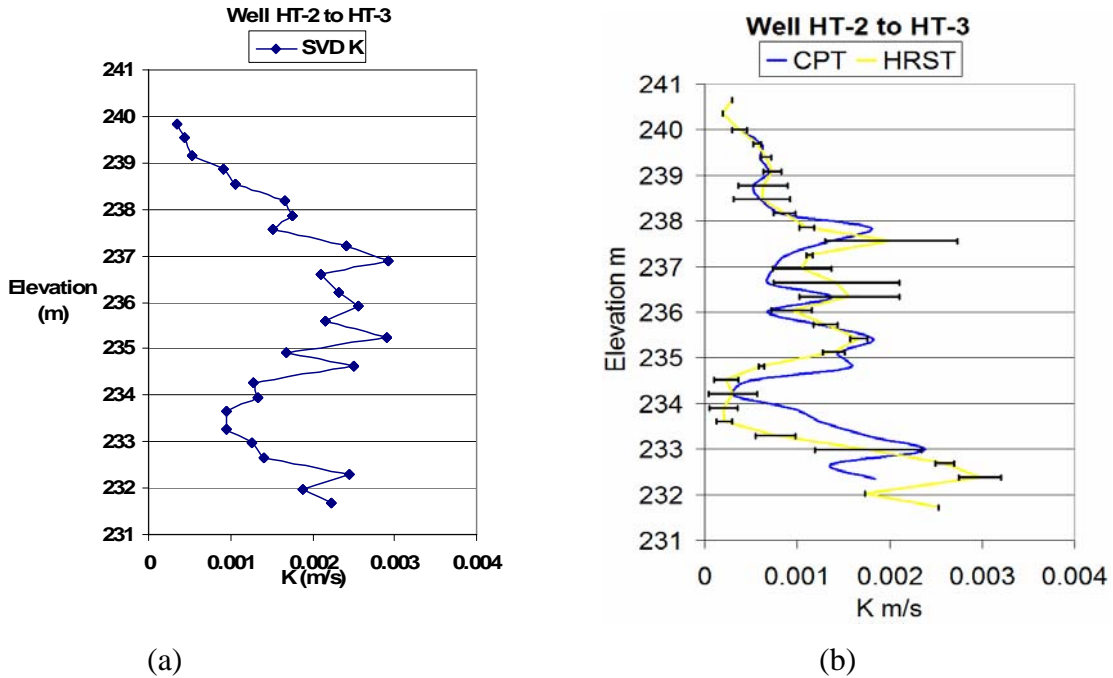


Figure 19. Comparison of K values obtained by horizontal rays in the SVD program (a) and K values obtained by CPT and HRST methods (b).

The resolution limit of the inversion model has been shown to be roughly 0.9144 m (3 ft). One run through of the model produced only a third of the K values presented above. Data in this particular well pair was collected at a finer scale than could be accounted for by the inverse model resolution, resulting in a lot of unused data. The problem was circumvented by running the inverse model three times. The initial model went to the bottom of the screened interval. Every run had the same element spacing and total depth, but each successive run positioned the bottom depth 0.30 m shallower than the previous run. The K values from the three individual runs were combined together to provide a higher resolution than initially expected from the inversion model.

New Wells Installed

In late October of 2007, three additional wells were added to GEMS. The wells were chosen to provide better coverage of the area under study by hydraulic tomography. The wells were installed using the direct push method with a Geoprobe unit from the Kansas Geological Survey. In the direct push method, metal drive casing is driven directly into the ground using a combination of hydraulics and percussive force. After one section of drive casing is pushed into the ground, an additional section of casing is screwed onto the previous section to proceed deeper (Figure 20). Once the desired depth is reached, the hollow outer metal drive casing holds the hole open while the PVC casing for the well is inserted in the middle. Each well had the bottom 10.67 m (35 ft) screened with 20 slot screen, meaning that each slot is .020 in (0.000508 m) in width (Figures 21 and 22). After insertion of the 2 in (.05 m) PVC casing, it is necessary to anchor the PVC casing in place while the metal drive casing is pulled up. In pulling up on the drive casing, a disposable pointed tip that sealed the end of the drive casing is pushed out and left at the bottom of the hole. The advantage of direct push over other drilling methods is that the area around the hole is less disturbed (Thornton et al., 1997). However, there is a possibility of water and material rushing in and binding the PVC casing inside the drive casing when the drive casing is removed. This problem was alleviated by filling the hole with water pumped from another well at GEMS while removing the first 6.1 m (20 ft) of drive casing. The water maintains pressure around the open end of the drive casing and keeps sand from entering. Once the casing had been completely removed, the annulus around the well was first filled in with sand to a point above the water level, and then

backfilled with bentonite to within a short distance of the surface. Surface material can be used to make a cleaner finish at the surface.



Figure 20. Direct push installation of the new wells.

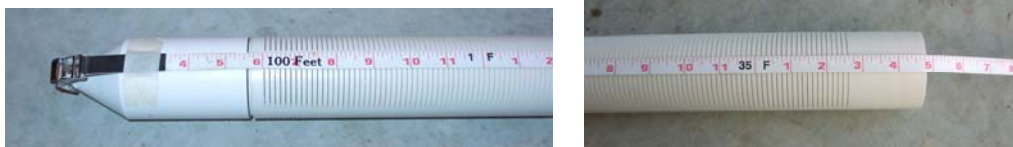


Figure 21. Slotted PVC casing used in the new wells.



Figure 22. Installation of casing in new wells.

After installing the wells, they were purged and developed to ensure a proper connection with the aquifer. Total depth measurements indicated that aquifer material had flowed into each well through the screen, reducing the total depth by as much as half a meter. One week after installation, the wells were pumped using a method called air lifting to develop the wells and to remove some of this extra sediment. An air compressor is connected to a hose placed inside the well. Air is channeled through the bottom of the hose and pushes water and sediment out through the top of the well. A shroud is used where the air exits at the bottom of the hose to prevent the air from going

directly into the aquifer. The hose was dropped to the bottom of the well and then was pulled up in 0.46 m (1.5 ft) increments. The hose was pulled up 24 times for a total of 11 m (36 ft) to develop the entire length of screen. A total depth measurement after air lifting the first well indicated that material was still present in the bottom of the well, possibly due to sediment entering the well after the hose was raised to shallower locations. The air lifting alone failed to remove all of the sediment, so a bailer was successfully used to remove the remainder. A bailer is simply a cylinder with a one-way check valve in the bottom. When dropped in a well, water and sediment fill in the bailer through the valve. As the bailer is pulled back up, the valve closes to hold the water and sediment in place until they can be poured out at the surface.

The week following the air lifting, the entire water column of each well was pneumatically oscillated for one hour per well. The period of the oscillation was within the range of periods used for data collection of the MOGs. The oscillation allowed water, and therefore also sediment, to move into and out of the well. After oscillating, total depths were measured again and some sediment had entered the bottom of the well. The bailer was used for about an hour on each well to remove the excess sediment and achieve the proper total well depth.

Following water column oscillation and bailing, wells were pumped using a submersible pump. The first well pumped, HT-4, was pumped starting at the top of the screened interval until the water was mostly clear of sediment. The pump was then dropped incrementally to the bottom of the well. The pumping was started at the top of the screen in an attempt to avoid sediment binding up the pump. In spite of attempts to avoid it, the pump did bind up with sediment when sitting on the bottom of the well. Air

lifting was resumed for 40-50 minute periods at the bottom of each new well to try and remove some of the sediment. Following a disassembly and cleaning of the pump in the lab, it was taken back out and placed a few feet below the water level, but above the top of the screen. For the first two wells pumped, HT-4 and HT-5, the pump shut off periodically due to electrical problems, but each time would restart immediately. Continuing problems with the pump required that we borrow an identical pump from the Kansas Geological Survey to finish pumping the wells. Each of the new wells was pumped for 40-45 minutes. Total depth measurements were taken to ensure that the wells remained clean. At this point, we felt the wells had been developed sufficiently and were ready for data collection.

As mentioned earlier, the new well locations were chosen to give good coverage of the area selected for study by hydraulic tomography. The wells initially installed for this project were HT-1, HT-2 and HT-3. The new wells are HT-4, HT-5, and HT-6. All of these wells as well as some others previously used for hydraulic tomography work are shown below in Figure 23. After installation and development, the wells were surveyed to establish the elevation of the top of each casing. Also, various radii between wells were measured for future analysis of the cross-well data. All of this information about the various wells that may be used in this tomographic study is shown in Table 1.

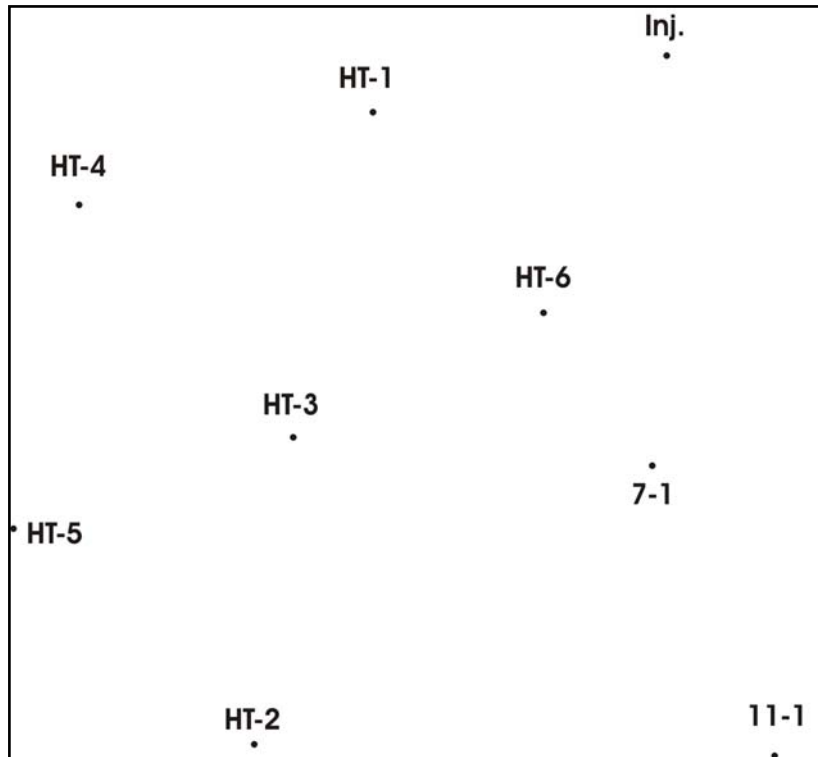


Figure 23. Relative well locations at GEMS (North is up). This shows the locations of the new wells installed in Oct. 2007, in addition to older wells previously used in this study.

Table 1. Well Information

Location	Elevation ft	Elevation m	Depth ft	Depth m	Screen ft	Screen m
Stake	827.556	252.239	-----	-----	-----	-----
HT-1	830.005	252.986	72.3	22.04	35.0	10.67
HT-2	829.66	252.880	72.4	22.07	35.0	10.67
HT-3	829.705	252.894	~70.	~21.3	35.0	10.67
HT-4	830.129	253.023	72.2	22.01	35.0	10.67
HT-5	829.651	252.878	71.9	21.92	35.0	10.67
HT-6	830.272	253.067	~72.	~21.9	35.0	10.67
7-1	828.342	252.479	68.85	20.99	30.0	9.14
11-1	828.358	252.484	69.40	21.16	45.0	13.72
Inj. Well	829.794	252.921	71.09	21.67	34.0	10.36

Well to Well Radial Distances, r

Well	Well	Radius (m)	Radius (ft)
HT-3 to	HT-1	4.77	15.65
HT-3 to	HT-2	4.36	14.31
HT-3 to	HT-4	4.46	14.62
HT-3 to	HT-5	4.21	13.81
HT-3 to	HT-6	3.99	13.10
HT-6 to	7-1	2.70	8.85
HT-6 to	11-1	7.19	23.58
HT-6 to	Inj. Well	4.04	13.26
Inj. Well to	HT-1	4.28	14.05
Inj. Well to	HT-4	8.67	28.45
Inj. Well to	HT-5	11.55	37.89
Inj. Well to	HT-2	11.49	37.70
Inj. Well to	HT-3	7.66	25.15
7-1 to	HT-2	6.94	22.79
7-1 to	HT-5	9.18	30.10
7-1 to	HT-3	5.13	16.84
7-1 to	HT-4	9.00	29.53
7-1 to	HT-1	6.46	21.20
HT-6 to	HT-1	3.79	12.42
HT-1 to	HT-4	4.40	14.44
HT-4 to	HT-5	4.63	15.21
HT-5 to	HT-2	4.57	15.00
HT-2 to	HT-6	7.40	24.28

HRST

A slug test gives an average of the hydraulic conductivity values in the vicinity of a well. Traditional slug tests use the entire well and therefore provide an average of K values throughout the whole well. High resolution slug testing (HRST) provides greater vertical resolution than whole well slug tests because the K value is only averaged over a small interval between the packers, which can be as low as 0.075 m (3 in) (Healey et al., 2004). A slug test is performed by increasing or decreasing the water level and observing the recovery to static water level. The water level change can be achieved by either adding or removing water or by adding or removing a solid object from the well. Pneumatic slug testing methods are increasingly being used. The procedure is the same as in the continuous pulse test. The water column can be depressed with air pressure and then allowed to return to its static level.

After installation and development of the new wells, high resolution slug testing (HRST) was performed on each of the new wells to establish the vertical distribution of hydraulic conductivity at that well. This information will be integrated into the analysis of the cross-well hydraulic tomography later. HRST uses some of the same equipment as the MOGs, but modified slightly for a the slug tests. A nitrogen-inflated double packer system is used to isolate a small portion of the well. A pump, able to supply pressure or vacuum, is connected to the well to either lower or raise the water level. Pressure transducers were used to measure both the air pressure and the water pressure. At each location four slug tests are performed with differing initial head; the initial head conditions used were +2.44, -2.44, +1.22, and -2.44 m (+8, -8, +4, and -8 ft). After

establishing these initial head conditions, a valve was opened to release the pressure or vacuum and start the slug test. There were 30 locations measured in each well with 0.3 m (1 ft) spacing to span the length of the screened interval. Pictures of the recording and initiation phases of the HRST are shown in Figures 24 and 25. Processing of this HRST data will be a high priority in the coming weeks.



Figure 24. Recording phase of HRST.



Figure 25. Initiation phase of HRST.

MOGs in New Wells

Multiple offset gathers (MOGs) were taken with the source in each of the three new wells and the receiver in well HT-3 (Figure 23). The receiver was kept in the same well to maximize data collection before winter. The source was moved in 0.91 m (3 ft) intervals for all three source wells. For the first well, HT-6, the receiver was moved in 0.30 m (1 ft) intervals. To expedite data collection in wells HT-4 and HT-5, the receiver was moved in 0.91 m intervals. The different intervals in each well will be compared to their resolution capabilities. If the larger intervals can provide equally good resolution, then less data will need to be collected in future MOGs at the site. This data has only received preliminary processing at this time; but, this is an area of continuing effort.

Summary and Conclusions

We have looked at the possibility of extending the simple homogeneous analytical solutions to heterogeneous situations. Modeling studies were performed since we do not have analytical solutions for general heterogeneous situations. The modeling work indicates a useful extension of the homogeneous formulas is possible, making interpretation of the heterogeneous data more efficient and without introducing much approximation error. We have used a straight ray-path approximation with a weighted average of the aquifer properties over that ray path. The predicted amplitudes and phases of the approximation agree well with the results of a numerical model of the heterogeneous aquifer. We have used a singular value decomposition (SVD) method to perform a least squares inverse of the straight ray-path approximation data to find the hydraulic conductivity (K) distribution. The data presented in this paper suggests that zones on the order of one meter (3 feet) square should be resolvable, but stability problems can occur without taking into account issues of spatially variable resolution and random error.

Development of the vertical sensor array has continued. After several problems have been solved, we seem to have a good workable version of the vertical sensor array. It has been used to collect a number of cross-well profiles, which can be used for hydraulic tomography processing.

Three new wells were installed at GEMS for this project. The locations were chosen to give some lateral extension to the area being studied. The wells were installed with direct push technology, which causes less aquifer disturbance than many other methods. The 22 m (70 ft) deep wells were fitted with .05 m (2 in) PVC casing and with

11 m (35 ft) of screen at the bottom. These wells were extensively developed to prepare them for data collection. High resolution slug testing (HRST) was performed on each of the wells at .30 m (1 foot) intervals. Three additional cross-well surveys were performed measuring the phase and amplitude variations between HT-3 and the new wells.

Processing of zero offset profile (ZOP) field data (obtained with the vertical sensor array) using the SVD method has yielded K values that compare well to those obtained by other methods used at the site. Preliminary processing of the multiple offset gather (MOG) data with the SVD inversion routines has experienced some instability problems due to model configuration and ambient noise. We continue to work on this problem. It is anticipated that additional work on configuring the model and conditioning the inverse with the HRST results will yield stable and reasonable inverse results. In summary, the use of oscillatory pressure waves for hydraulic tomographic reconstruction of hydraulic conductivity distributions using the spatially weighted raypath method shows promise. This research was supported in part by the U.S. Department of Defense, through the Strategic Environmental Research and Development Program (SERDP).

References

- Aster, R.C., Borchers, B., and Thurber, C.H., 2005, Parameter Estimation and Inverse Problems, Elsevier Academic Press, Burlington, MA.
- Barker, J.A., 1988. A generalized radial flow model for hydraulic tests in fractured rock. *Water Resources Research* 24. No. 10:1796-1804.
- Black, J.H., and Kipp, K.L. 1981. Determination of hydrogeological parameters using sinusoidal pressure tests: A theoretical appraisal. *Water Resources Research* 17. No. 3:686-692.
- Bohling, G.C., 1999. Evaluation of an induced gradient tracer test in an alluvial aquifer, Ph.D. Dissertation, University of Kansas, 224 p.
- Bohling, G.C., Zhan, X., Knoll, M.D., Butler J.J. Jr. 2003. Hydraulic tomography and the impact of a priori information: An alluvial Aquifer Example. *Kansas Geological Survey Open-file Report 2003-71*
- Brauchler, R., Liedl, R., Dietrich, P., 2001. A travel time based hydraulic tomographic approach. *Water Resources Research* 39. No. 12:1-12
- Bredehoeft, J.D and Papadopoulos, S.S. 1980. A method for determining the hydraulic properties of tight formations. *Water Resources Research* 16. No. 1:233-238
- Cooper, H.H., Bredehoeft, J.D., Papadopoulos, I.S., and Bennett, R.R. 1965. The response of well-aquifer systems to seismic waves. *Journal of Geophysical Research* 70, No. 16:3915-3926
- Engard, B., 2006, Estimating Aquifer Parameters From Horizontal Pulse Tests, Masters Thesis, University of Kansas, 107 pp.
- Engard, B., McElwee, C.D., Healey, J.M., and Devlin, J.F., 2005, Hydraulic tomography and high-resolution slug testing to determine hydraulic conductivity distributions – Year 1: Kansas Geological Survey Open File Report #2005-36, 81 p.
- Engard, B.R., McElwee, C.D., Devlin, J.F., Wachter, B., and Ramaker, B., 2006, Hydraulic tomography and high-resolution slug testing to determine hydraulic conductivity distributions – Year 2: Kansas Geological Survey Open-File Report # 2007-5, 57 pp.
- Ferris, J.G., 1951. Cyclic fluctuations of the waterlevels as a basis for determining aquifer transmissivity, *IAHS Publ.*, 33, p. 148-155.

- Hantush, M.S., 1960. Lectures at New Mexico Institute of Mining and Technology. unpublished, compiled by Steve Papadopoulos, 119 p.
- Healey, J., McElwee, C., and Engard, B., 2004. Delineating hydraulic conductivity with direct-push electrical conductivity and high resolution slug testing. *Trans. Amer. Geophys. Union* 85, No.47: Fall Meet. Suppl., Abstract H23A-1118.
- Huettl, T.J., 1992. An evaluation of a borehole induction single-well tracer test to characterize the distribution of hydraulic properties in an alluvial aquifer. Masters Thesis, The University of Kansas.
- Jiang, X., 1991. Field and laboratory study of the scale dependence of hydraulic conductivity. Masters Thesis, The University of Kansas.
- Jiao, J.J. and Tang, Z., 1999. An analytical solution of groundwater response to tidal fluctuation in a leaky confined aquifer. *Water Resources Research* 35. No. 3:747-751
- Johnson, C.R., Greenkorn, R.A., and Woods, E.G., 1966. Pulse-Testing: A new method for describing reservoir flow properties between wells. *Journal of Petroleum Technology*. (Dec1966) pp. 1599-1601.
- Lee, J., 1982. Well Testing. Society of Petroleum Engineers of AIME, New York. 156 p.
- McCall, W., Butler J.J. Jr., Healey, J.M., and Garnett, E.J., 2000. A dual-tube direct push method for vertical profiling of hydraulic conductivity in unconsolidated formations. *Environmental & Engineering Geoscience* Vol. VIII, no. 2:75-84
- McElwee, C.D., 2001. Application of a nonlinear slug test model. *Ground Water* 39. No. 5:737-744
- McElwee, C.D., 2002. Improving the analysis of slug tests. *Journal of Hydrology* 269:122-133
- McElwee, C.D., and Butler, J.J. Jr., 1995. Characterization of heterogeneities controlling transport and fate of pollutants in unconsolidated sand and gravel aquifers: Final report. Kansas Geological Survey open file report 95-16.
- McElwee, C.D., and Zenner, M.A., 1998. A nonlinear model for analysis of slug-test data. *Water Resources Research* 34. No. 1:55-66.
- Novakowski, K.S., 1989. Analysis of pulse interference tests. *Water Resources Research* 25. No. 11:2377-2387
- Pierce, A., 1977. Case history: Waterflood performance predicted by pulse testing. *Journal of Petroleum Technology*. (August 1977) 914-918.

Ross, H.C. 2004. Utility of multi-level slug tests to define spatial variations of hydraulic conductivity in an alluvial aquifer, northeastern Kansas. Masters Thesis, The University of Kansas.

Ross, H.C. and McElwee, C.D., 2007, Multi-level slug tests to measure 3-D hydraulic conductivity distributions. *Natural Resources Research*, DOI: 10.1007/s11053-007-9034-9.

Schad, H., and Teutsch, G., 1994. Effects of scale on pumping test results in heterogeneous porous aquifers. *Journal of Hydrology* 159. pp. 61- 77.

Schulmeister, 2000. Hydrology and geochemistry of an alluvial aquifer near a flood plain margin. Dissertation, University of Kansas.

Sellwood, S., 2001. A direct-push method of hydrostratigraphic site characterization. Masters thesis, The University of Kansas.

Thorton, D., S. Ita, and K. Larsen. 1997, Broader use of innovative ground water access technologies, In Proceedings of Superfund XVIII Conference, vol. 2.

Van Der Kamp, G.,1976. Determining aquifer transmissivity by means of whole well respons tests: The underdamped case. *Water Resources Research* 12. No. 1:71-77.

Yeh, T.C., and Liu, S., 2000. Hydraulic tomography: Development of a new aquifer test method. *Water Resource Research* 36. No. 8:2095-2105

Zemansky, G.M., and McElwee, C.D., 2005. High-Resolution Slug Testing. *Ground Water* 43. No. 2: 222-230

Appendix A. Technical Publications

Published Abstracts.

Healey, J. M., McElwee, C. D., and Engard, B., 2004, Delineating hydraulic conductivity with direct push electrical conductivity and high-resolution slug testing: *Eos, Trans. Amer. Geophys. Union*, v. 85, no 47, Fall Meet. Suppl., Abstract H23A-1118, p. F773.

Engard, B. and McElwee, C. D., 2005, Continuous pulse testing for estimating aquifer parameters: *Proceedings 50th Annual Midwest Ground Water Conference*, Nov. 1-3, Urbana, Illinois.

Engard, B. and McElwee, C. D., 2005, Estimating aquifer parameters from oscillatory well stresses: *Proceedings SERDP Partners in Environmental Technology Technical Symposium and Workshop*, Nov. 29-Dec. 1, Washington, D.C., p. G-26.

Engard, B. and McElwee, C. D., 2005, Estimating hydraulic conductivity: Hydraulic tomography and high-resolution slug tests: *Eos, Trans. Amer. Geophys. Union*, 86(52), Fall Meet. Suppl., Abstract H21C-1359.

McElwee, C. D. and Engard, B., 2006, Using Oscillatory Pressure Waves to Measure Hydraulic Conductivity Distributions: *Proceedings SERDP Partners in Environmental Technology Technical Symposium and Workshop*, Nov. 28-30, Washington, D.C.

McElwee, C. D. and Engard, B., 2006, Hydraulic Tomography Using Oscillatory Pressure Waves: *Eos, Trans. Amer. Geophys. Union*, 87(52), Fall Meet. Suppl., Abstract H41B-0382.

McElwee, C. D., 2007, Hydraulic Conductivity Distributions from Pulsed Signals: Mini-Symposium 45 – Tomographic Approaches to High-Resolution Aquifer Characterization – Lab and Field Experiments, SIAM Conference on Mathematical & Computational Issues in the Geosciences, March 19-22, Santa Fe, NM.

McElwee, C. D. and Wachter, B. J., 2007, A Modeling Study Using Oscillatory Pressure Waves for Hydraulic Tomography: *Eos, Trans. Amer. Geophys. Union*, 88(23), Joint Assembly Suppl., Abstract H51E-01.

McElwee, C. D. and Wachter, B. J., 2007, Oscillatory Pressure Waves as Energy Source for Hydraulic Tomography: *Proceedings SERDP Partners in Environmental Technology Technical Symposium and Workshop*, Dec. 4-6, Washington, D.C.

Wachter, B. J. and McElwee, C. D., 2007, Hydraulic Tomography Study Involving the Singular Value Decomposition Method: *Eos, Trans. Amer. Geophys. Union*, 88(52), Fall Meet. Suppl., Abstract H23G-1725.

Annual Report

Engard, B., McElwee, C.D., Healey, J.M., and Devlin, J.F., 2005, Hydraulic tomography and high-resolution slug testing to determine hydraulic conductivity distributions – Year 1, Project Report to the Strategic Environmental Research and Development Program, U.S. DoD, EPA, and DOE, 81 pp., also Kansas Geological Survey Open File Report #2005-36.

Engard, B.R., McElwee, C.D., Devlin, J.F., Wachter, B., and Ramaker, B., 2006, Hydraulic tomography and high-resolution slug testing to determine hydraulic conductivity distributions – Year 2, Project Report to the Strategic Environmental Research and Development Program, U.S. DoD, EPA, and DOE, 57 pp., also Kansas Geological Survey Open-File Report # 2007-5.

Masters Thesis

Engard, B., 2006, Estimating Aquifer Parameters From Horizontal Pulse Tests, Masters Thesis, University of Kansas, 107 pp.